

CHARACTERIZATION OF L-CYSTEINE SOURCES USING ATR-FTIR AND RAMAN SPECTROSCOPY

Z. MOHAMAD ZHARIF¹, T. NUR AZIRA^{2*}, A.S. MUHAMAD SHIRWAN³

International Institute for Halal Research and Training (INHART), International Islamic University Malaysia, Jalan Gombak, 53100 Kuala Lumpur, Malaysia.

**Corresponding author: aziratukiran@iium.edu.my*

(Received: 10th Nov. 2020, Accepted: 30th Dec. 2020, Published on-line: 15th Jan. 2021)

ABSTRACT: L-cysteine is a form of food additive that is commonly used in baking ingredients. It serves as a stabilizer to soften the texture of the dough. Unfortunately, the use of L-cysteine in the dough is a controversial issue as animal and human parts are highly likely to be its primary sources. This study aims to characterize the L-cysteine sources by using Attenuated Total Reflection Fourier Transform Infrared (ATR-FTIR) and Raman spectroscopy. Raw materials consisted of pig bristles, human hair, cow horn, duck feather and chicken feather were analysed. The result found that the ATR-FTIR is preferable rather than Raman spectroscopy in differentiating the primary sources of L-cysteine. Data pre-treatment was carried out to provide a more reliable analysis and good data interpretation. Accordingly, principal component analysis (PCA) transformed the transmittance of ATR-FTIR into several principal components (PCs). Five distinct groups were successfully differentiated in PCA. The proposed method offers a fast and environmentally friendly approach to distinguish the primary sources of L-cysteine. Hence, this method is beneficial to be used for origin determination of L-cysteine food additives.

KEYWORDS: *L-cysteine; Food additives; Raman spectroscopy; Attenuated Total Reflection Fourier Transform Infrared (ATR-FTIR); Principal Component Analysis (PCA)*

1. INTRODUCTION

L-cysteine is a part of amino acid composition to many proteins and enzymes. It is of interest due to the presence of a reactive thiol group as a side chain, (Demirkol et al., 2004; Helmutgmunder et al., 1990; Hunt, 1985). The thiol group involves in many control functionalization such as detoxification of heavy metals in living organisms, antioxidant capabilities of tissues and mitochondria, blood coagulation in mammals, transport across cell membranes and electrochemical sensing, (Cai et al., 2014; Cebi et al., 2017; Borase et al., 2015; Ensafi et al., 2009). L-cysteine is usually found in relatively low concentration in dietary protein which does not exceed 5% of total amino acids, (Demirkol et al., 2004; Ismail et al., 2014). They can be found in whole food such as meats, grains, nuts, fruits and vegetables.

The production of L-cysteine in worldwide market can reach up to 400 tons where the production is used as food additives, dietary supplements and pharmaceutical products, (Berehoiu et al., 2013; Jahangir et al., 2016). In food industry, L-cysteine acts as stabilizer in bakery products by softening the texture of the yeast and preventing further oxidation, while in animal food production it is used as artificial flavor by mimicking meat flavor, (Ismail et al., 2014; Wu, 2013; Wada & Takagi, 2006). However, the primary sources of L-cysteine are controversial issue as there is a chance it is derived from animal and human parts such as human hair, cow horn, pig bristles and duck feather, (Cai et al., 2014; Ismail et al., 2014). This raised an ethical issue and concerns on the *halal* integrity upon the sources of the raw materials especially among Muslim consumers. According to the fatwa released by Department of Islamic Development Malaysia (JAKIM), any type of food that is derived from the human body (hair) is considered as haram (MS1500, 2009). Hence, there is an urgent need for implementing a reliable approach to characterize the sources of L-cysteine.

Current approaches for L-cysteine sources differentiation include spectroscopic, spectrophotometric and analytical methods with advanced gold determination applications, (Zulkarnail et al., 2020). These methods offer advantages in terms of sensitivity, efficiency and short period of time. Nonetheless, some of these approaches are somewhat complex and expensive. Therefore, a method that is robust, requires short period of sample preparation and easily interpreted should be considered.

Recently, the vibrational spectroscopy methods which are Attenuated Transform Fourier Infrared (ATR-FTIR) and Raman spectroscopy have gained attention due to their abilities to determine the chemical fingerprinting and chemical profiling. Precisely, most functional groups can be observed in mid-infrared ATR-FITR spectroscopy (wavelength 4000 to 400 cm^{-1}) since their vibrational resonances fall within this range of excitation frequencies, (Gordon, 2011). On the other hand, Raman spectroscopy is assigned based on the spectral positions, intensities and polarizations of the Raman bands which are sensitive to protein secondary, tertiary and quaternary structures, as well as to side-chain orientations along with local environments, (Nemecek et al., 2013). They serve as complementary and confirmatory analysis for a lot of samples. For example, polar functional groups can be detected better in ATR-FTIR, whereas aromatic carbon bond (e.g. C=C and C-H) can be easily excited with Raman spectroscopy, (Käppler et al., 2016). In fact, both vibrational spectroscopic analysis have become the advanced approaches for meat species identification based on the chemical fingerprinting profiling with the known sample without targeting specific molecule, (Cebi et al., 2017; Ramin Jorfi, 2012). In addition, ATR-FTIR and Raman spectroscopy offer numerous advantages such as rapid analysis, simple use and low cost of sample preparation, (Hashim, 2013; Nemecek et al., 2013; Ramin Jorfi, 2012). However, the spectra from both spectroscopic methods need further data transformation approach as the spectrums might be too complex or weak. Thus, chemometrics tool is required to evaluate the data and produce feasible results.

Principal component analysis (PCA) is one of the chemometrics tool to illustrate data into simplest form. Precisely, PCA could reduce the dimensionality of a data collection by representing only significant information, (Nemati et al., 2004). A study conducted by Gok et al. (2015), proved that a combination of spectral analysis ATR-FTIR and chemometrics test was able to discriminate a total of 144 honey floral sources based on their geographical origins. Other than that, ATR-FTIR spectroscopy had been demonstrated to be successful for differentiation of *Triticum* and its closely related genus, *Aegilops*, (Demir et al., 2015). PCA is also able to distinguish Arabica and Robusta coffee by using Raman spectra range between 2700 to 3050 cm^{-1}

¹, (El-Abassy, Donfack & Materny, 2011). The combination of Raman spectroscopy and PCA can be used to determine food adulteration in butter and margarine, (Uysal et al., 2013). This study aims to investigate the spectral fingerprint on each sample based on ATR-FTIR and Raman spectroscopy. Moreover, PCA is performed to monitor the classification as a graphical display to determine the relationship between each source. Therefore, a stepwise L-cysteine authentication approach can be developed and implemented by legal authority to determine the *halal* integrity of L-cysteine additives used in food industry.

2. MATERIALS AND METHOD

2.1 Materials and Chemicals

Five different sources of L-cysteine were analysed (i.e., human hair, pig bristles, duck feather, chicken feather and cow horn). Human hair was collected at a local barbershop while pig bristles (PB) and duck feather (DF) were obtained from Department of Wildlife and National Parks (PERHILITAN). Meanwhile, chicken feather (CF) and cow horn (CH) were collected from local wet market in Selangor, Malaysia.

6M Hydrochloric acid was obtained from Merck KGaA (Darmstadt, Germany). L-cysteine hydrochloride standard was obtained from Sigma Aldrich Malaysia with Chemical Abstract Service (CAS) number 52-89-1. Tap water was also used in the experiment.

2.2 Sample Preparation and Extraction of L-cysteine Sources

All samples were thoroughly washed with tap water and afterwards, dried in the oven at 37°C overnight. One gram of each sample was mixed with 6M HCl and incubated in the oven for 24-hours at 110°C. Subsequently, samples were freeze-dried for three days to obtain dried powder samples. The powder samples were then analysed with spectral analysis tools.

2.3 Raman Spectroscopy Measurements

Renishaw inVia Raman microscope system (Renishaw, Wotton) objective lens was used for measurements. The measurements were collected with 10-second exposure time and one accumulation by using 20 times magnification. The samples were scanned in extended range of 400 to 2100 cm^{-1} with 1 cm^{-1} spectral resolution for triplicates reading. WiRE 4.0 software (Renishaw, UK) was used to focus on the spot. The Raman spectra for each sample were recorded and analysed.

2.4 Attenuated Total Reflection Fourier Transform Infrared (ATR FT-IR)

Spectra were collected in the one-bounce ATR mode in a Spectrum 100 FTIR spectrometer (Perkin-Elmer Inc., Norwalk, CT, USA) equipped with a Universal ATR accessory. Approximately 0.5g of each sample was placed on Diamond/ZnSe crystal plate (Perkin-Elmer, United Kingdom) and scanned from 4000 to 650 cm^{-1} with resolution of 4 cm^{-1} at air condition room temperature 20-22°C. The samples were analysed thrice. Three times data analysis were carried out via Spectrum 100 software (Perkin-Elmer, United Kingdom).

2.5 Statistical analysis

Spectra data from ATR-FTIR were validated by using XL Stat software version 7.5.2 (Addinsoft, New York, USA). Box plot analysis was applied to remove any outlier data from samples spectra. Kaiser-Meyer-Olkin (KMO) was administered to determine the construct validity and measure the sampling adequacy. Principal Component Analysis (PCA) was used as data reduction method. In this work, PCA was conducted on the ATR-FTIR spectra at the wavenumber region between $4000\text{--}650\text{ cm}^{-1}$, $1700\text{--}1600\text{ cm}^{-1}$, $1175\text{--}940\text{ cm}^{-1}$ and $940\text{--}700\text{ cm}^{-1}$ range

3. RESULTS AND DISCUSSION

3.1 Raman Spectroscopy Analysis

Figure 1 shows the Raman spectra of different sources of L-cysteine (CF, CH, PB, HH and DF) at wavenumber region between the range of 190 cm^{-1} – 1010 cm^{-1} . This range was selected as Raman band of S-S and could be observed at 495 cm^{-1} , (Kodera et al., 2017) while S-H groups of cysteine could be observed at 500 cm^{-1} – 510 cm^{-1} , (Nemecek et al., 2013). Figure 2 shows L-cysteine amino acid standard in Raman spectroscopy. The spectrum exhibited one prominent peak at approximately 500 cm^{-1} . This peak or element may provide a reliable and direct interpretation of Raman spectrum. Compared to Figure 1, there was no Raman shift peak recorded on all samples except for CH. There was one peak recorded at approximately 900 cm^{-1} . However, the peak was too weak to be assigned for specific compound. In addition, fluorescence spectra were recorded for the remaining samples (PB, CH, CF and DF). Nevertheless, the changes of polarizability on each sample were either too weak or undesired fluorescence superpose the Raman spectra which hinder compound identification, (Chen et al., 2014; Ferrer et al., 2011; Marshall & Copper, 2016). Therefore, the data from Raman spectroscopy were not further analyzed by PCA for classification of sources.

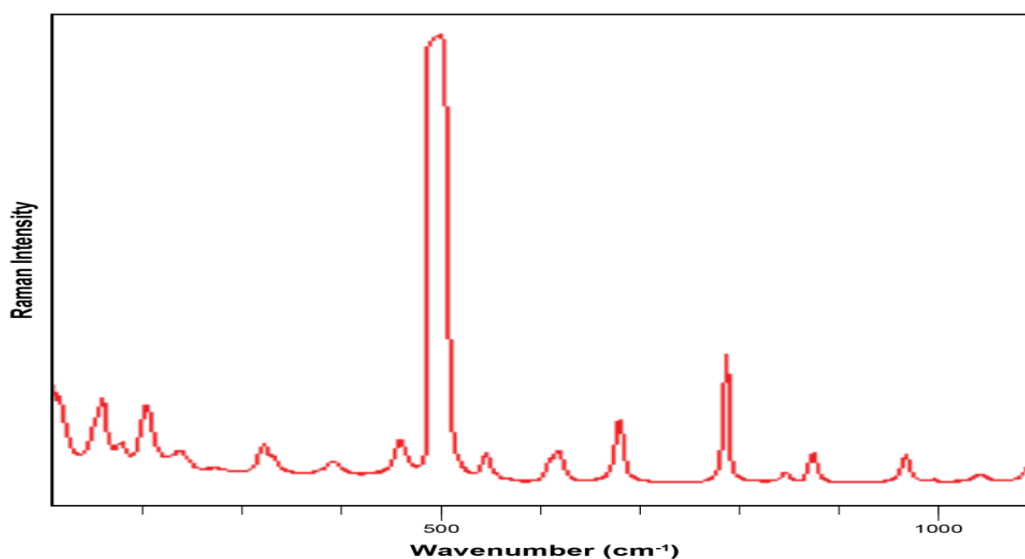


Fig. 1: Raman spectrum of L-cysteine amino acid at wavenumber 190 cm^{-1} – 1010 cm^{-1} .

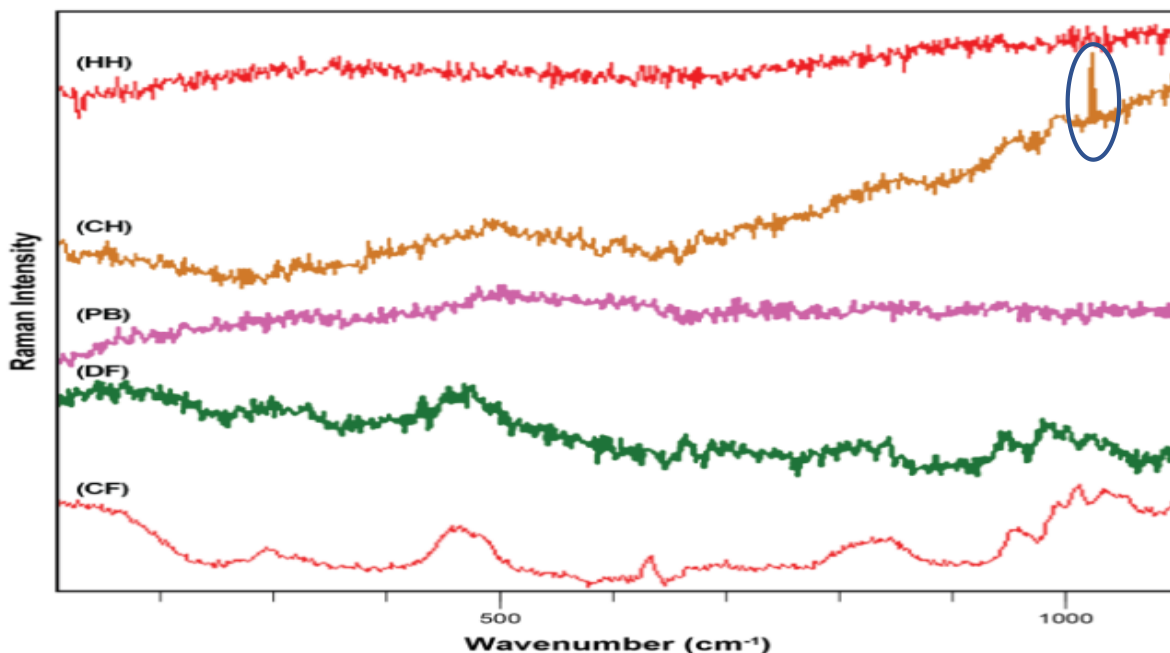


Fig. 2: Raman spectra of CF, DF, PB, CH and HH at wavenumber $190\text{cm}^{-1} - 1010\text{cm}^{-1}$.

3.2 Fourier Transform Infrared (FTIR) Spectroscopy Analysis

Fig. 3 shows the FTIR spectra of different sources of L-cysteine (CF, CH, PB, HH and DF) at wavenumber region between the range of $4000\text{cm}^{-1} - 1000\text{cm}^{-1}$. These spectra displayed the typical characteristic of absorption bands for common protein. The analytical evaluation of different L-cysteine sources is presented in Table 1. The entire range of spectra looks similar for all L-cysteine sources to the naked eyes. This is due to the similar chemical composition of protein compound. However, when the spectra are examined closely, minor differences between each spectra of L-cysteine sources are detected. The differences can be observed on amide band at frequency of $1550\text{cm}^{-1} - 1600\text{cm}^{-1}$ caused by N-H bending and secondary effect of C-N stretch, (Amir et al., 2013; Vongsvivut et al., 2014).

The spectra on Fig. 3 shows that the amide band for CF was located at 1556cm^{-1} , HH at 1559.05cm^{-1} , in the range of $1580.18\text{cm}^{-1} - 1556.38\text{cm}^{-1}$ for CH and PB at 1566.95cm^{-1} . Meanwhile, there was no recorded absorption of amide band in DF sample. In contrast, the prominent band of L-cysteine standard was observed at 1402cm^{-1} (Fig. 4), whereas for CH, it was assigned at 1398.21cm^{-1} region, and for PB as well as CF, the bands were spotted at 1403cm^{-1} and 1430.78cm^{-1} respectively. The spectra feature showed that CF and PB were significantly different as opposed to other samples. There were similar spectra appeared at $1550\text{cm}^{-1} - 1350\text{cm}^{-1}$ in all samples, indicating the existence of N-H_{bend} , $\text{C-N}_{\text{stretching}}$, $\text{C-C}_{\text{stretching}}$, $\text{COO}_{\text{asymmetric}}$, $\text{COO}_{\text{symmetric}}$, (Chen et al., 2018; Koyun & Sahin, 2018). On the other hand, the bands appeared between wavenumber of $1700\text{cm}^{-1} - 1650\text{cm}^{-1}$ indicate the presence of C=O and C-N, (Hashemi et al., 2017; Bai et al., 2014).

Table 1: Transmittance value of ATR-FTIR from five L-cysteine sources CF, CH, DF, HH and PB.

Samples	1050.72	1217.31	1315.64	1403.78	1455.29	1536.84	1556.68	1643.99	1659.5	1797.23	1951.91	1980.18	2036.56	2050.18	2072.38	2099.05	2112.35	2150.11	2162.26	2185.53	2257.77	2285.54	2323.5	2349.01	2455.01	2626.71	2780.93	2834.09	2881.01	3284.8	3416
CF I	97.1	97.3	97.4	97.2	97.4	97.1	97.0	96.9	96.9	97.5	97.3	96.6	96.6	96.6	97.0	97.1	97.0	97.2	96.0	96.5	96.9	96.8	97.1	97.6	97.2	97.1	97.4	0.0	97.7	96.6	0.0
CF II	97.3	97.6	97.6	97.3	97.6	97.2	97.1	96.9	96.9	97.8	97.5	96.7	96.8	96.8	97.2	97.2	97.3	97.5	96.2	96.7	97.1	97.0	97.3	97.9	97.5	97.4	97.7	97.8	97.9	96.7	0.0
CF III	97.4	97.7	97.7	97.5	97.7	97.3	97.2	97.0	97.1	97.9	97.5	96.7	96.8	96.8	97.2	97.4	97.3	97.2	96.2	96.7	97.0	97.3	97.4	97.8	97.6	97.6	97.9	97.9	98.1	96.8	0.0
CF II II	97.6	97.9	97.9	97.8	98.0	97.7	97.6	97.4	97.4	98.1	97.7	96.9	96.9	97.1	97.5	97.6	97.6	97.6	96.4	96.9	97.4	97.4	97.5	98.0	97.8	97.7	98.0	98.1	98.2	97.1	0.0
CF II III	96.8	97.0	97.0	96.9	97.2	96.9	96.8	96.7	96.7	97.1	96.7	96.0	96.0	96.1	96.5	96.6	96.5	96.5	95.8	96.0	96.4	96.4	96.6	97.0	96.8	96.8	97.1	97.2	97.5	96.4	0.0
CF III I	97.6	97.9	97.9	97.8	98.0	97.7	97.7	97.5	97.5	98.2	97.8	97.1	97.2	97.3	97.6	97.7	97.6	97.7	97.2	97.1	97.4	97.4	97.7	98.1	97.8	97.8	98.1	98.1	98.3	97.2	0.0
CF III II	97.7	97.9	98.0	97.9	98.1	97.8	97.8	97.6	97.6	98.3	98.0	97.1	97.3	97.2	97.6	97.8	97.7	97.8	97.2	97.1	97.4	97.4	97.6	98.2	97.9	97.9	98.1	98.2	98.4	97.1	0.0
CF III III	96.6	96.9	96.9	96.6	96.9	96.5	96.4	96.1	96.1	97.1	96.7	95.7	96.1	96.1	96.4	96.5	96.5	96.6	95.3	95.9	96.3	96.3	96.5	97.1	96.7	96.7	96.9	96.9	97.3	95.9	0.0
CH I	98.6	98.4	97.5	95.3	97.0	0.0	93.2	93.2	0.0	99.6	99.2	98.5	98.4	98.4	98.7	98.8	98.7	98.8	97.7	98.2	98.4	98.3	98.4	98.7	0.0	97.7	0.0	96.8	96.3	93.0	0.0
CH II	98.4	0.0	97.3	94.9	96.7	0.0	92.6	92.5	0.0	99.6	98.9	98.0	98.0	98.4	98.4	98.5	98.5	98.4	97.2	97.8	98.2	98.2	98.3	98.6	0.0	97.5	0.0	96.6	95.9	93.0	0.0
CH II II	98.6	0.0	97.8	95.9	97.3	0.0	94.1	94.1	0.0	99.5	99.0	98.4	98.3	98.4	98.6	98.6	98.7	98.7	97.7	98.1	98.4	98.4	98.5	98.9	98.4	97.9	0.0	97.3	96.8	95.2	0.0
CH II III	98.4	0.0	97.1	94.4	96.5	0.0	91.9	91.8	0.0	99.5	99.0	98.2	98.4	98.2	98.5	98.6	98.5	98.5	97.4	97.9	98.2	98.1	98.1	98.3	98.0	97.3	0.0	96.3	95.6	92.8	0.0
CH III I	98.5	0.0	97.3	95.0	96.8	0.0	92.8	92.5	0.0	99.5	99.1	98.3	98.4	98.3	98.6	98.6	98.6	98.6	97.9	98.0	98.3	98.2	97.4	97.6	98.2	0.0	0.0	96.8	96.3	93.1	0.0
CH III II	98.4	0.0	97.5	95.5	97.0	0.0	93.6	93.6	93.7	99.5	98.9	98.0	98.0	98.0	98.4	98.5	98.5	98.4	97.1	97.7	98.2	98.2	98.5	98.9	98.3	97.7	0.0	97.1	96.6	94.6	0.0
CH III III	98.6	0.0	97.5	95.5	97.0	0.0	93.5	93.2	93.3	99.5	99.0	98.2	98.2	98.2	98.5	98.6	98.5	98.5	97.3	97.9	98.3	98.2	98.3	98.8	98.2	97.6	0.0	97.0	96.4	93.7	0.0
CH III II II	98.4	0.0	97.1	94.8	95.6	0.0	92.6	92.3	0.0	99.5	99.0	98.2	98.1	98.1	98.4	98.5	98.5	98.4	97.2	97.8	98.1	98.1	98.0	98.4	98.1	97.4	0.0	95.6	96.0	92.8	0.0
CH III III	99.3	0.0	97.8	95.7	97.2	0.0	93.4	93.2	93.3	99.9	99.4	98.5	98.5	98.5	98.8	98.9	98.9	99.0	97.7	98.3	98.6	98.5	98.4	98.8	98.5	97.8	0.0	97.0	96.3	94.0	0.0
DF I	98.7	98.7	98.6	98.3	98.3	0.0	97.7	92.6	93.4	98.9	98.1	97.0	97.0	97.0	97.4	97.5	97.5	97.5	96.2	96.9	97.7	97.7	98.2	98.5	98.5	98.6	0.0	98.6	98.5	0.0	73.8
DF II	98.8	0.0	98.8	0.0	98.5	98.0	0.0	92.0	0.0	99.1	98.3	97.4	97.2	97.1	97.6	97.7	97.7	97.7	96.5	97.1	97.8	97.9	98.4	99.0	98.7	98.8	98.9	98.8	98.6	0.0	71.8
DF II I	98.8	0.0	98.9	0.0	98.5	0.0	0.0	93.2	0.0	99.1	98.3	97.3	97.2	97.2	97.7	97.8	97.8	97.7	98.5	97.2	97.9	98.1	98.3	99.0	98.7	98.8	98.9	98.8	98.6	0.0	75.9
DF II II	98.8	98.8	98.8	0.0	98.5	98.2	98.1	93.8	94.5	99.1	98.4	97.6	97.6	97.5	97.8	97.9	98.0	98.0	96.8	97.4	98.0	98.1	98.4	98.9	96.7	98.7	98.9	98.7	98.6	0.0	77.8
DF II III	99.0	99.0	99.0	0.0	98.6	0.0	98.0	92.9	99.2	99.2	98.5	97.6	99.3	97.3	97.8	97.9	97.9	97.8	96.5	97.2	98.0	98.1	98.5	99.1	96.9	98.9	99.0	98.9	98.8	0.0	73.7
DF III I	98.7	99.0	99.1	98.3	98.7	0.0	97.4	94.2	94.7	99.5	98.7	97.6	97.6	97.7	98.2	98.3	98.3	98.1	96.8	97.5	98.2	98.3	98.7	99.2	98.9	98.8	98.8	98.7	98.4	0.0	80.3
DF III II	98.7	98.9	98.9	98.4	98.7	98.2	97.9	95.3	95.8	99.1	98.4	97.6	97.5	97.6	98.0	98.1	98.1	97.9	96.8	97.4	98.0	98.1	98.5	99.0	98.7	98.4	98.8	98.7	98.6	0.0	83.5
DF III III	98.9	0.0	98.9	98.5	98.8	98.4	98.1	96.3	96.6	99.0	98.3	97.4	97.4	97.5	97.9	98.0	98.0	97.8	96.8	97.3	97.9	98.1	98.4	98.9	98.6	98.6	98.7	98.7	98.7	0.0	87.4
DF III II II	98.6	0.0	99.0	98.6	98.8	0.0	0.0	96.3	0.0	99.1	98.2	97.2	97.2	97.3	97.8	97.9	97.9	97.7	96.4	97.1	97.8	98.0	98.3	98.9	98.6	98.6	98.8	98.7	98.6	0.0	87.8
HH I	98.4	0.0	98.5	98.0	98.3	0.0	96.9	95.0	0.0	98.8	98.0	97.0	97.0	97.0	97.6	97.7	97.7	97.6	96.2	96.9	97.6	97.8	98.0	0.0	98.3	98.3	0.0	98.4	98.2	0.0	84.2
HH II	98.6	98.8	0.0	98.2	98.5	97.9	97.5	95.5	95.7	99.0	98.4	97.5	97.6	97.6	98.0	98.0	98.0	98.1	96.9	97.4	97.9	98.0	98.3	98.8	98.5	98.5	98.6	98.5	98.4	0.0	84.9
HH II I	98.7	98.9	98.8	98.4	98.6	0.0	97.5	95.3	0.0	99.1	98.3	97.3	97.3	97.4	97.9	98.0	98.0	97.8	96.6	97.2	98.0	98.1	98.4	0.0	98.7	98.7	98.7	98.7	98.5	0.0	84.2
HH II II	98.6	98.7	98.5	98.1	98.1	98.0	0.0	92.9	0.0	98.7	97.0	96.9	96.9	96.9	97.4	97.4	97.5	97.4	96.2	96.9	97.6	97.7	98.0	98.6	98.5	98.5	98.7	98.5	98.5	0.0	74.1
HH II III	98.6	99.2	99.0	98.5	98.4	0.0	97.8	92.9	0.0	99.3	98.6	97.6	97.4	97.5	97.9	98.0	98.0	98.1	96.7	97.4	98.2	98.3	98.5	99.2	99.0	99.0	99.2	98.8	98.5	0.0	73.2
HH III I	98.5	99.0	98.8	0.0	98.3	0.0	0.0	96.1	96.5	99.0	98.2	97.3	97.3	97.3	97.8	98.0	97.9	97.7	96.6	97.1	97.9	98.0	98.4	98.9	98.5	98.5	98.5	98.4	98.3	0.0	85.8
HH III II	98.3	98.7	98.5	0.0	98.1	98.4	98.1	96.8	97.0	98.8	98.2	97.4	97.4	97.4	97.8	97.9	97.9	97.9	97.7	97.3	97.7	97.7	98.6	98.6	98.2	98.2	98.2	98.1	98.2	0.0	89.1
HH III III	98.2	98.4	98.2	97.8	97.8	0.0	0.0	93.0	0.0	98.5	97.8	96.8	96.7	96.8	97.2	97.3	97.3	97.3	96.1	96.7	97.4	97.4	97.7	98.3	98.2	98.2	98.3	98.3	98.2	0.0	75.4
HH III II II	98.4	98.6	98.5	97.9	98.2	0.0	0.0	93.9	0.0	98.9	98.3	98.0	97.3	97.3	97.7	97.8	97.8	98.0	96.6	97.2	97.8	97.8	98.0	98.7	98.5	98.4	98.5	98.4	98.2	0.0	80.1
PB I	97.8	0.0	98.2	98.1	98.3	98.1	98.1	98.1	98.2	0.0	96.7	96.7	96.8	97.3	97.4	97.4	97.2	96.2	96.6	97.2	97.3	97.6	98.2	97.8	0.0	98.3	98.4	98.5	97.9	98.2	
PB II	97.7	0.0	98.2	98.2	98.2	0.0	98.1	0.0	98.0	98.2	97.5	96.5	96.6	96.7	97.2	97.4	97.4	97.1	95.9	96.5	97.2	97.3	97.7	98.2	97.9	0.0	98.3	98.4	98.5	97.9	97.9
PB II I	97.9	98.3	98.5	98.4	98.5	0.0	98.3	97.8	97.9	98.6	98.0	97.2	97.3	97.3	0.0	97.8	97.8	97.7	96.6	97.1	97.6	97.6	98.0	98.5	98.2	0.0	98.5	98.5	98.6	96.0	95.1
PB II II	97.8	98.1	98.2	98.1	98.2	98.1	98.1	97.7	97.7	98.3	97.7	96.9	96.9	97.0	97.4	97.5	97.5	97.4	96.2	96.8	97.4	97.4	97.8	98.3	98.0	98.1	98.4	98.5	98.5	0.0	95.8
PB II III	0.0	0.0	98.3	98.3	98.4	98.3	98.2	97.9	98.0	98.5	97.7	96.7	96.8	96.9	97.4	97.6	97.6	97.3	96.2	96.8	97.5	97.6	97.8	98.4	98.1	0.0	98.6	98.5	98.6	97.4	97.3
PB III I	97.8	97.1	98.2	98.2	98.3	0.0	98.1	98.0	98.1	98.3	97.5	96.6	96.6	96.8	97.3	97.5	97.5	97.2	96.0	96.6	97.3	97.4	97.7	98.2	98.0	0.0	9				

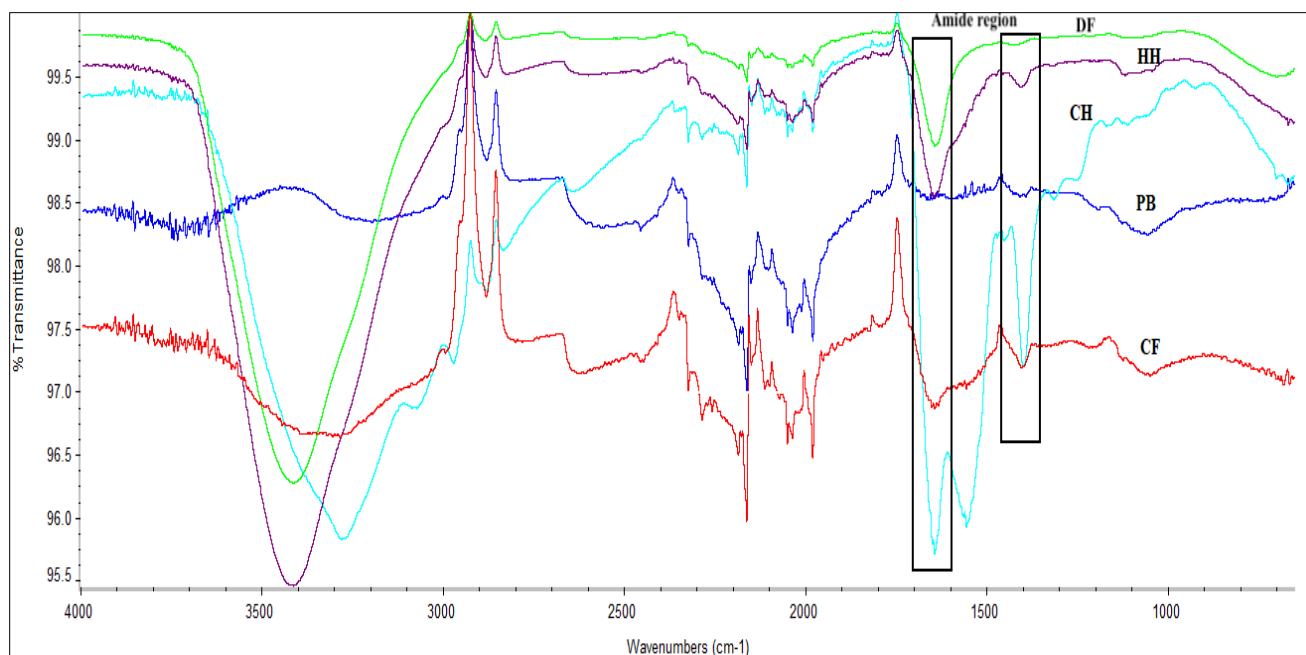


Fig. 3: Collection of ATR-FTIR from five different types of samples (DF, HH, CH, PB and CF).

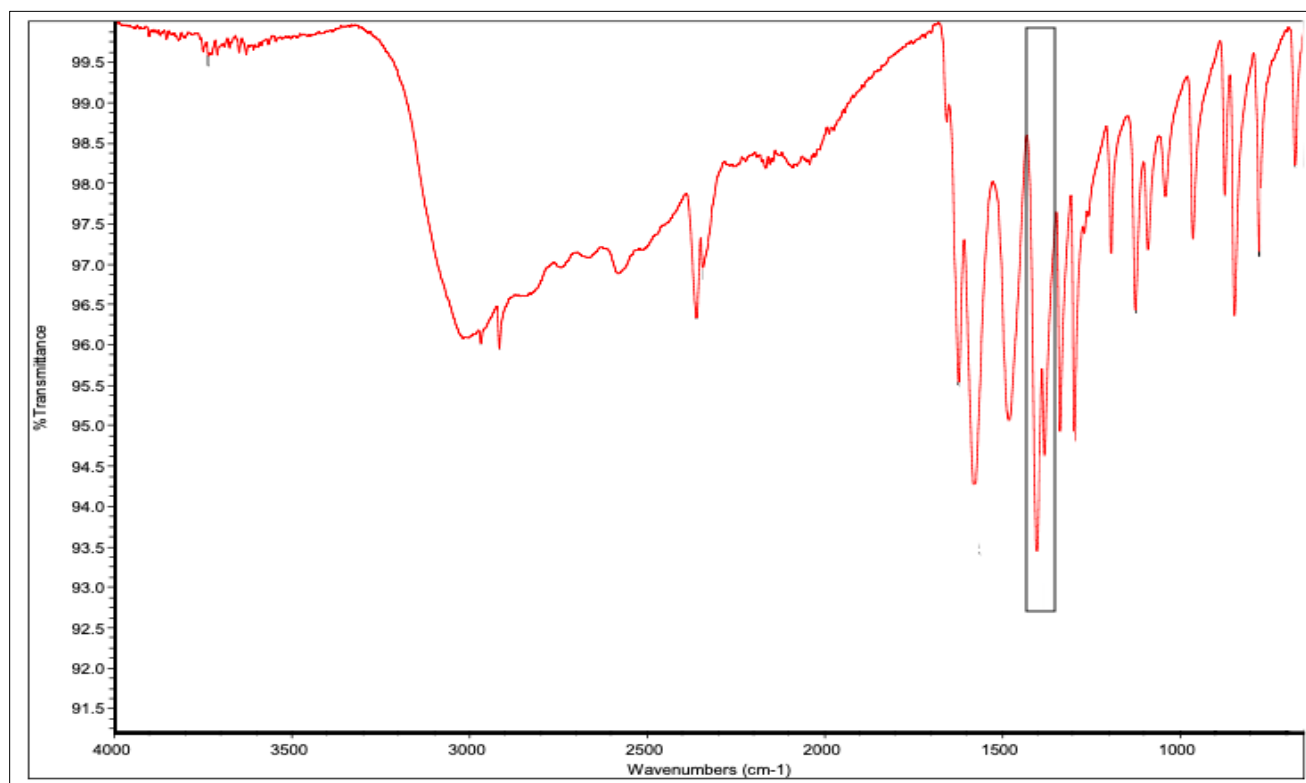


Fig. 4: Spectrum of L-cysteine standard.

3.3 Data Pre-processing

Data pre-processing is a required procedure to determine the reliability of the data obtained from the tested sample in ATR-FTIR. This is to ensure the suitability of the data to be proceeded with the principal component analysis (PCA). A series of tests was conducted to determine the reliability of the data acquired from the tested samples. For example, KMO test is used to determine the adequacy of the data, (Bertsch, 2012). On the contrary, Barlett test and eigenvalue are used to determine the outlier and strong correlation between each sample respectively, (Engel et al., 2013). Hence, pre-processed data is administered in this experiment to confirm the reliability of the data from ATR-FTIR.

Combination of chemometrics test is advantageous to determine the underlying relationship between each variable. The spectral fingerprint between each sample could be described in the simplest way with the aid of PCA. Each sample could be discriminated with respect to their spectral fingerprint based on the data obtained from ATR-FTIR and Raman Spectroscopy.

3.3.1 Data Validity and Reliability

A stepwise approach was taken prior to interpret the data in PCA to determine the reliability of the data obtained. A box plot test was carried out to remove the outlier transmittance. The remaining transmittance from all samples were tested with KMO and Barlett test. Based on Table 2 the transmittance data show KMO = 0.7348 which is (>0.5) and Barlett test score showed Cronbach's alpha = 0.8436 (>0.05) which is relatively significant. The Barlett test score proved that correlations between variables were significantly different.

Table 2: Preprocessing test value of FTIR transmittance data.

Items	Cronbach's alpha	KMO	Barlett test of sphericity
Transmittance	0.8346	0.7348	.005

The transmittance value between each sample were further validated prior to being applied in PCA. Based on Table 2, the eigenvalue of F1 and F2 components were 12.9447 and 2.1152 respectively. These two components showed higher cumulative variance which are 80.9043 in F1 and 94.1245 in F2. In order to determine the underlying relationship between each FTIR transmittance value, factor loading of more than 0.75 were selected to be used in PCA. Table 4 showed that 16 ATR-FTIR transmittances had a value above 0.75. This shows that the data had the highest correlation in F1 and F2 components. Hence, the result proved that the selected transmittance value was reliable to be used in PCA.

Table 3: Eigenvalue and cumulative variance of FTIR transmittance.

	F1	F2
Eigenvalue	12.9447	2.1152
Cumulative Variance	80.9043	94.1245

Table 4: Factor loading table of FTIR transmittance in each sample.

	F1	F2
1315.64	0.3743	0.8889
1556.68	0.9220	0.2493
1643.99	0.8096	0.1619
1797.23	0.9450	0.3073
1951.91	0.9586	0.0550
1980.18	0.9503	0.0387
2036.56	0.9755	0.1938
2050.18	0.9746	0.1806
2072.38	0.9867	0.0829
2099.05	0.9767	0.0689
2112.35	0.9824	0.0547
2150.11	0.9659	0.1542
2185.53	0.9869	0.1058
2257.77	0.9594	0.2532
2285.54	0.9044	0.4044
2780.93	0.3800	0.8890

3.4 Differentiation of L-cysteine Sources by PCA

All samples were further analyzed with PCA where they were grouped based on the ATR- FTIR transmittance. Fig. 5 shows that the samples were successfully separated into five distinct groups. L-cysteine sources of DF, HH and CH were separated on positive F1. Meanwhile, PB and CF almost shared the same group on negative F2. Hence, it shows that the combination of ATR-FTIR and PCA were able to characterize the samples into different groups.

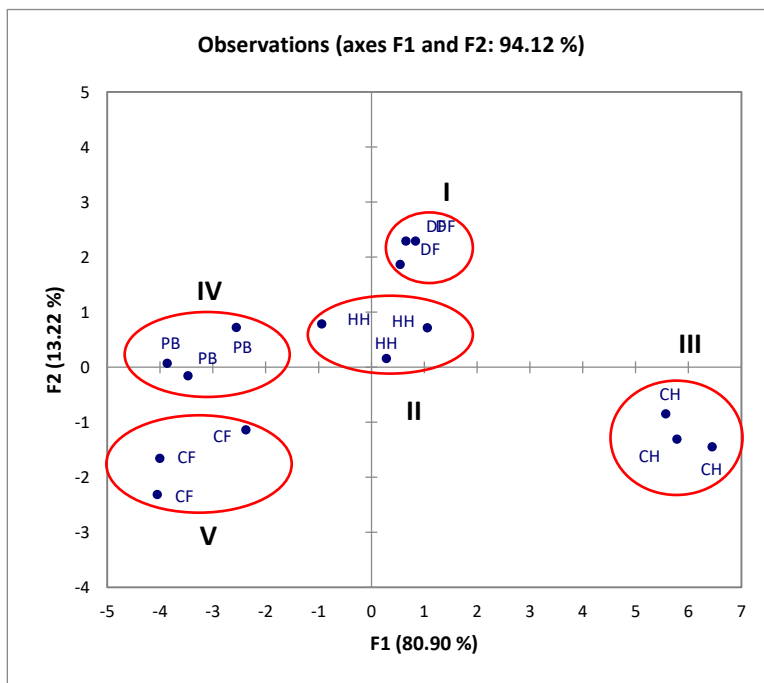


Fig. 5: PCA score plot of chicken feather (CF), duck feather (DF), cow horn (CH), pig bristles (PB) and human hair (HH).

A variable plot is used to determine the ATR-FTIR transmittance that responds to the grouping of the sample. Based on Fig. 6, a large part of ATR-FTIR transmittance was located on positive F1 which was close to CH grouping sample. Meanwhile, the transmittance value of 1556.68 and 1643.99 were in PB samples. This could be used as a specific transmittance identification marker for PB grouping sample. On the other hand, it can be seen that 2780.93 was corresponded to duck feather sample. HH samples were strongly correlated to the origin of variable plot and the grouping for CH did not show any transmittance value. The variable plot proved that, transmittance value in ATR-FTIR was successfully used to differentiate the sample into five distinct groups in PCA.

3.5 Halal Industry

The global *halal* market is expected to expand due to the increase in consumer demand. In order to maintain the integrity of *halal* market, lawful ingredients and quality of food products should be taken seriously by the authorities and experts of the industry. Therefore, to meet the industrial demand, a fast and reliable authentication approach is required to identify and assert the lawful ingredients. This study proposed a tier approach for protein authentication. A fast and robust analysis by ATR-FTIR can capture the fingerprinting profiles for all L-cysteine sources. In fact, the combination of PCA showed that the L-cysteine sources can be differentiated into specific groups and interpreted easily. Thus, the proposed method is credible to be used as a guideline for any L-cysteine additives used in the baking ingredients or confectionery products available in the market.

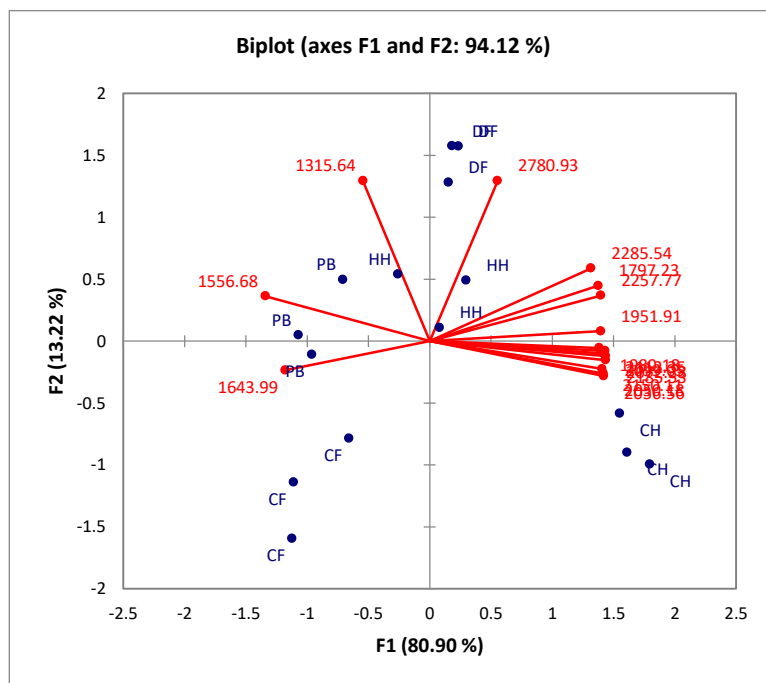


Fig. 6: PCA Variable plots of ATR FTIR transmittance in L-cysteine sources.

4. CONCLUSION

Differentiation of L-cysteine sources can be developed through the combination of ATR-FTIR and PCA. The experiment showed that ATR-FTIR were successfully illustrated the spectral band of all L-cysteine sources. Finding highlight the interpretation of transmittance value in ATR-FTIR successfully detected of L-cysteine sources. This can be seen when ATR-FTIR can identify the presence of amide I and amide II band in all samples. In fact, with a combination of ATR-FTIR transmittance and PCA, all samples were successfully being separated into a specific group. Nevertheless, the experiment can further elucidate by modifying sample preparation method exclusively for Raman analysis. Thus, a reliable authentication method could be developed based on the chemical composition of the raw materials.

REFERENCES

- [1] Amir, R. M., Anjum, F. M., Khan, M. I., Khan, M. R., Pasha, I., & Nadeem, M. (2013). Application of Fourier transform infrared (FTIR) spectroscopy for the identification of wheat varieties. *Journal of Food Science and Technology*, 50(5), 1018–1023. <https://doi.org/10.1007/s13197-011-0424-y>
- [2] Bai, B., Chen, L. L., Li, Q. L., Duan, Y. Q., Liu, L., Tan, D. H., & Ji, S. J. (2014). Preparation and functional exploration of cysteine peptides from fresh garlic scales for improving bioavailability of food legume iron and zinc. *Chinese Journal of Analytical*

- Chemistry, 42(10), 1507–1512. [https://doi.org/10.1016/S1872-2040\(14\)60776-3](https://doi.org/10.1016/S1872-2040(14)60776-3)
- [3] Berehoiu, R. M. ., Popa, C. N., & Popescu, S. (2013). Assessment of the E 920 Additive (L - Cysteine) in Relation To Some Problems of Modern Food Industry. *Scientific Papers Series Management, Economic Engineering in Agriculture and Rural Development*, 13(1), 413–418.
- [4] Bertsch, A. M. (2012). Validating GLOBE ’ s Societal Values Scales : A Test in the U . S . A . *International Journal of Business and Social Science*, 3(8), 10–24. <https://doi.org/10.1002/ijop.12100>
- [5] Cai, X., Li, J., Zhang, Z., Wang, G., & Song, X. (2014). Talanta Chemodosimeter-based fluorescent detection of L -cysteine after extracted by molecularly imprinted polymers. *Talanta*, 120, 297–303. <https://doi.org/10.1016/j.talanta.2013.12.019>
- [6] Cebi, N., Dogan, C. E., Develioglu, A., Yayla, M. E. A., & Sagdic, O. (2017). Detection of L-Cysteine in wheat flour by Raman microspectroscopy combined chemometrics of HCA and PCA. *Food Chemistry*, 228, 116–124. <https://doi.org/10.1016/j.foodchem.2017.01.132>
- [7] Demir, P., Onde, S., & Severcan, F. (2015). Phylogeny of cultivated and wild wheat species using ATR-FTIR spectroscopy. *Spectrochimica Acta - Part A: Molecular and Biomolecular Spectroscopy*, 135, 757–763. <https://doi.org/10.1016/j.saa.2014.07.025>
- [8] Demirkol, O., Adams, C., & Ercal, N. (2004). Biologically important thiols in various vegetables and fruits. *Journal of Agricultural and Food Chemistry*, 52(26), 8151–8154. <https://doi.org/10.1021/jf040266f>
- [9] El-Abassy, R. M., Donfack, P., & Materny, A. (2011). Discrimination between Arabica and Robusta green coffee using visible micro Raman spectroscopy and chemometric analysis. *Food Chemistry*, 126(3), 1443–1448. <https://doi.org/10.1016/j.foodchem.2010.11.132>
- [10] Engel, J., Gerretzen, J., Szymańska, E., Jansen, J. J., Downey, G., Blanchet, L., & Buydens, L. M. C. (2013). Breaking with trends in pre-processing? *TrAC - Trends in Analytical Chemistry*, 50, 96–106. <https://doi.org/10.1016/j.trac.2013.04.015>
- [11] Ensafi, A. A., Rezaei, B., & Nouroozi, S. (2009). Flow injection spectrofluorimetric determination of cystine and cysteine. *Journal of the Brazilian Chemical Society*, 20(2), 288–293.
- [12] Gok, S., Severcan, M., Goormaghtigh, E., Kandemir, I., & Severcan, F. (2015). Differentiation of Anatolian honey samples from different botanical origins by ATR-FTIR spectroscopy using multivariate analysis. *Food Chemistry*, 170, 234–240. <https://doi.org/10.1016/j.foodchem.2014.08.040>
- [13] Hashim, M. (2013). *SCIENCE & TECHNOLOGY A Review of Cosmetic and Personal Care Products : Halal Perspective and Detection of Ingredient*. *Pertanika J. Sci. & Technol*, 21(May 2011), 281–292. <http://www.pertanika.upm.edu.my/>
- [14] Helmutgmunder, H.-P., Benninghoff, B., & Roth, S. (1990). Macrophages Regulate Intracellular Glutathione Levels of Lymphocytes. Evidence for an Immunoregulatory Role of Cysteine’. *Cellular Immunology*, 129, 32–46. [https://doi.org/10.1016/0008-8749\(90\)90184-S](https://doi.org/10.1016/0008-8749(90)90184-S)
- [15] Hunt, S. (1985). Degradation of Amino Acids Accompanying in vitro Protein Hydrolysis, Chap. 12. *Chemistry and Biochemistry of the Amino Acids*, 376–397.
- [16] Jahangir, M., Mehmood, Z., Saifullah, Bashir, Q., Mehboob, F., & Ali, K. (2016). Halal status of ingredients after physicochemical alteration (Istihalah). *Trends in Food Science and Technology*, 47, 78–81. <https://doi.org/10.1016/j.tifs.2015.10.011>
- [17] Käßpler, A., Fischer, D., Oberbeckmann, S., Schernewski, G., Labrenz, M., Eichhorn, K., &

- Voit, B. (2016). Analysis of environmental microplastics by vibrational microspectroscopy : FTIR , Raman or both? *Analytical and Bioanalytical Chemistry*, 8377–8391. <https://doi.org/10.1007/s00216-016-9956-3>
- [18] Koyun, O., & Sahin, Y. (2018). Poly(L-cysteine) modified pencil graphite electrode for determination of sunset yellow in food and beverage samples by differential pulse voltammetry. *International Journal of Electrochemical Science*, 13(1), 159–174. <https://doi.org/10.20964/2018.01.40>
- [19] Nemecek, D., Stepanek, J., & Thomas, G. J. (2013). Raman spectroscopy of proteins and nucleoproteins. *Current Protocols in Protein Science*. <https://doi.org/10.1002/0471140864.ps1708s71>
- [20] Ramin Jorfi. (2012). Differentiation of pork from beef, chicken, mutton and chevon according to their primary amino acids content for halal authentication. *African Journal of Biotechnology*, 11(32), 8160–8166. <https://doi.org/10.5897/AJB11.3777>
- [21] Uysal, R. S., Boyaci, I. H., Genis, H. E., & Tamer, U. (2013). Determination of butter adulteration with margarine using Raman spectroscopy. *Food Chemistry*, 141(4), 4397–4403. <https://doi.org/10.1016/j.foodchem.2013.06.061>
- [22] Vongsivut, J., Heraud, P., Zhang, W., Kralovec, J. A., McNaughton, D., & Barrow, C. J. (2014). Rapid Determination of Protein Contents in Microencapsulated Fish Oil Supplements by ATR-FTIR Spectroscopy and Partial Least Square Regression (PLSR) Analysis. *Food and Bioprocess Technology*, 7(1), 265–277. <https://doi.org/10.1007/s11947-013-1122-8>
- [23] Wada, M., & Takagi, H. (2006). Metabolic pathways and biotechnological production of L-cysteine. *Applied Microbiology and Biotechnology*, 73(1), 48–54. <https://doi.org/10.1007/s00253-006-0587-z>
- [24] Wu, G. (2013). Functional amino acids in nutrition and health. *Amino Acids*, 45(3), 407–411. <https://doi.org/10.1007/s00726-013-1500-6>
- [25] Zulkarnail, M. Z., Tukiran, N. A., Sani, M. S. A., & Ismail, A. M. (2020). Recent advanced techniques in cysteine determination: A review. *Food Research*, 4(December), 2336–2346.